DOI: 10.1002/cssc.201100635

Regeneration of Silica-Supported Silicotungstic Acid as a Catalyst for the Dehydration of Glycerol

Benjamin Katryniok,*[a] Sébastien Paul,[a] Mickaël Capron,[b] Virginie Bellière-Baca,[c]
Patrick Rey,[d] and Franck Dumeignil[b, e]

The dehydration reaction of glycerol to acrolein is catalyzed by acid catalysts. These catalysts tend to suffer from the formation of carbonaceous species on their surface (coking), which leads to substantial degradation of their performances (deactivation). To regenerate the as-deactivated catalysts, various techniques have been proposed so far, such as the co-feeding of oxygen, continuous regeneration by using a moving catalytic bed, or alternating between reaction and regeneration. Herein, we study the regeneration of supported heteropolyacid catalysts. We show that the support has a strong impact on the thermal stability of the active phase. In particular, zirconia has been found to stabilize silicotungstic acid, thus enabling the nondestructive regeneration of the catalyst. Furthermore, the addition of steam to the regeneration feed has a positive impact by hindering the degradation reaction by equilibrium displacement. The catalysts are further used in a periodic reaction/regeneration process, whereby the possibility of maintaining long-term catalytic performances is evidenced.

Introduction

Limited petrol resources have inspired researchers to propose biomass-based substitutes for gasoline, diesel, and kerosene.[1–3] Although the environmental impact of biofuels in terms of carbon dioxide emissions is rather controversial, many nations have decided to promote the blending of commercial fuels with the aforementioned biomass-based compounds, such as biodiesel.[4] As a consequence, the production of the latter has significantly increased—especially in Europe. Biodiesel is produced by the transesterification of vegetable oils, which involves the production of large quantities of crude glycerol. Various valorization reactions have been described for this highly functionalized molecule (triol). Among them, the dehydration reaction to yield acrolein has attracted considerable attention because this compound is an intermediate widely used for the production of amino acids and superabsorbent polymers.[5,6] The dehydration reaction of glycerol is catalyzed by acid catalysts such as zeolites,[7,8] supported inorganic acids,[9–11] or mixed metal oxides.[12,13] Nevertheless, all of these catalytic systems suffer from a common drawback preventing stakeholders from envisioning any robust commercial applications because they are always subject to unavoidable deactivation by coke deposition.[10,11,14] As a consequence, and to compensate for the low stability of the catalytic systems, several processes have been proposed, based on the concept of a continuous regeneration, such as the co-feeding of oxygen,[13,15,16] the use of a circulating bed with separated reactor and regenerator,[17,18] or periodic regeneration by alternating the reactant and regeneration feeds.[19,20]

The first concept, based on co-feeding of oxygen, was initially proposed by Dubois et al. for zeolite catalysts loaded in a fixed-bed reactor and was further adapted for other types of catalysts.[15] Nevertheless, the main disadvantage of this type of process lies in the concomitant presence of oxygen and acrolein in the product flow, leading to the formation of undesired highly oxidized molecules, such as acrylic acid, acetic acid, or even carbon oxides, whereby the yield in acrolein generally decreases. Furthermore, the oxygen concentration in the flow must not surpass 7% to stay out of the explosive range of compositions. This implies that most of the reaction mixture consists of inert gas (nitrogen or steam), which decreases the overall productivity of the process.

The use of a circulating catalyst bed was first studied by Corma et al. in a fluid catalytic cracking (FCC)-type reactor with zeolite-based catalysts, whereby a constant and high yield of acrolein (60%) was obtained.[18] Furthermore, it was shown that the process could proceed autothermally because the heat released by coke combustion was recovered to evaporate

---

[a] Dr. B. Katryniok, Prof. S. Paul
Univ. Lille Nord de France, Ecole Centrale de Lille
Unité de Catalyse et de Chimie du Solide (UMR8181)
Cité Scientifique, F-59655 Villeneuve d'Ascq (France)
Fax: (+33) 320-33-54-99
E-mail: benjamin.katryniok@ec-lille.fr

[b] Dr. M. Capron, Prof. F. Dumeignil
Univ. Lille Nord de France, Université Lille 1
Unité de Catalyse et de Chimie du Solide (UMR8181)
Cité Scientifique, F-59655 Villeneuve d'Ascq (France)

[c] Dr. V. Bellière-Baca
RHODIA France
52 rue de la Haie Coq, 93308 Aubervilliers (France)

[d] Dr. P. Rey
ADISSEO France SAS
Antony Parc 2-10, 92160 Antony (France)

[e] Prof. F. Dumeignil
Institut Universitaire de France
10, Boulevard Saint-Michel, 75005 Paris (France)

Supporting Information for this article is available on the WWW under http://dx.doi.org/10.1002/cssc.201100635.

the glycerol solution. Nevertheless, the important investment costs of this method are surely one of the main drawbacks to be overcome before being able to scale this process up. Note that there are other drawbacks, such as the mechanical stress on the catalyst or the quantity of catalysts to be loaded into such a reactor.

Finally, the regeneration by alternating the reactant and regeneration feeds was used by Arita et al. for zeolite-type catalysts loaded in a fixed-bed reactor.[19] They proved that the initial catalytic performance was recovered, even if regeneration resulted in hot spots due to the exothermicity of coke combustion. Comparable results were also reported by Strohm et al.[20] Due to the straightforwardness and low investment costs needed to set this process up, it seems more favorable than co-feeding or circulating the catalyst bed, as long as the catalyst employed can resist the high regeneration temperature. The process can notably be performed by using two parallel reactors, whereby one works under reaction conditions and the other one under regeneration conditions (spare reactor); a technique already used for the catalytic reforming of naphtha (Figure 1).[21]

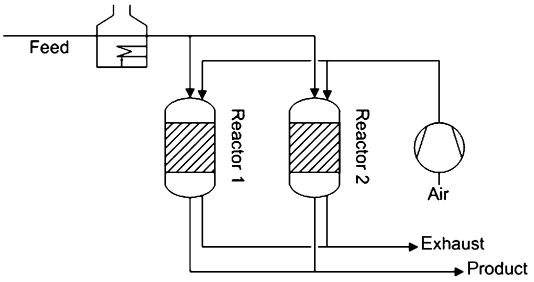

Figure 1. Process with a spare reactor similar to that used for the catalytic cracking of naphtha. (Adapted from Reference [20].)

Among the aforementioned three classes of catalysts—zeolites, mixed metal oxides and supported inorganic acids—the latter is widely studied, especially due to the facile control of the acidity and textural properties, which were both identified as the most important parameters to enable high catalytic performances in the dehydration of glycerol.[11,22] Whereas the textural properties are mainly a function of the catalyst support, the acid strength and the number of acid sites can directly be influenced through the quantity (density) and type of the active phase. Hereby, in particular, Keggin-type heteropolyacids (HPAs) were used because their acid strength is easily tunable by the choice of central and addenda atoms.[23,24] However, when considering the regeneration of these compounds by means of oxidative coke combustion, they largely suffer from their low thermal stability resulting in irreversible decomposition.[24,25]

We have recently demonstrated that the long-term catalytic performance of silicotungstic acid (STA) could already be substantially increased when supported on zirconia-grafted mesoporous silica.[26] Herein, we have focused on the oxidative regeneration of this type of catalyst using an alternating feed process and proved that combining the increased robustness of our novel catalytic system with a well-designed regeneration technology gives a powerful integrated solution for the sustainable production of acrolein by glycerol dehydration.

Results and Discussion

Characterization of fresh and spent catalysts

Nitrogen physisorption experiments

The catalysts containing 20 wt% STA on bare and zirconia-grafted SBA-15 were analyzed by nitrogen physisorption to determine their specific surface areas and their pore volume/size, and thereby, to assess the accessibility of the channels after impregnation and grafting. From the results given in Table 1, one can see that the impregnation of SBA-15 leads to a decrease in the specific surface area (431 vs. 541 m^2g^{-1}) and pore volume (1.05 vs. 1.20 cm^3g^{-1}), whereas the average pore diameter (8 nm) remains unchanged. The decrease in the specific surface area is in the range of 20%, which suggests that this decrease is only based on the increase in weight due to the introduction of the active phase. Due to the nonporous character of STA, the active phase introduced does not add any additional surface to the catalyst, whereby the specific surface area decreases proportionally to the amount of deposited active phase.

Table 1. Textural properties of supports and catalysts used.

Sample	S_{BET}[a] [m^2g^{-1}] ($S_{theo.}$[b] [m^2g^{-1}])	V_p[c] [cm^3g^{-1}]	D_p[d] [nm]
bare SBA-15	541	1.20	8
STA on SBA-15	431 (433)	1.05	8
ZrO_2 on SBA-15	465 (433)	1.15	8
STA on ZrO_2/SBA-15	378 (372)	0.68	7

[a] S_{BET} = BET specific surface area. [b] $S_{theo.}$ = theoretical specific surface area in reference to the initial support. [c] V_p = porous volume. [d] D_p = average pore diameter obtained by the BJH model.

Conversely, when SBA-15 is grafted with 20 wt% of zirconia, the decrease in specific surface area (465 vs. 541 m^2g^{-1}) and pore volume (1.15 vs. 1.20 cm^3g^{-1}) is less pronounced than in the aforementioned case of impregnation with the same amount of STA. This result can easily be explained by the porous nature of the grafted zirconia, whereby additional surface and porosity are generated on the SBA-15 host support. When the zirconia-grafted silica is further impregnated with 20 wt% of STA, the specific surface area decreases again by roughly 20% (378 vs. 465 m^2g^{-1}). Furthermore, we note a decrease in the pore volume (0.68 vs. 1.15 cm^3g^{-1}) and also in the pore diameter (7 vs. 8 nm). Nevertheless, the decrease in the latter is negligible and one can assume that the porous network remains essentially fully accessible to the reactant.

Acidity of fresh catalysts

The aforementioned catalysts and their corresponding supports were further analyzed by performing temperature-programmed desorption of NH_3 to determine the amount and strength of the acid sites. From the results gathered in Table 2, one can see that the bare SBA-15 support exhibits nearly no acid sites (0.004 mmol NH_3 uptake $g_{Cat.}^{-1}$). When the support is grafted with zirconia, the quantity of acid sites increases (0.178 mmol NH_3 uptake $g_{Cat.}^{-1}$) because zirconia is known to be a Lewis acid. By deconvolution of the thermograms, one can see that these sites are rather homogeneously distributed over the whole range of strengths (38% weak sites, 29% medium sites and 33% strong sites). Conversely, impregnation of the supports with STA leads to a significant increase in the number of acid sites because the HPA is a well-known Brønsted acid. Hereby, the catalyst based on SBA-15 exhibits NH_3 uptake of 0.339 mmol $g_{Cat.}^{-1}$ and the ZrO_2/SBA-15-based one of 0.442 mmol $g_{Cat.}^{-1}$. The stronger increase of the latter is attributed to only partial coverage of zirconia, whereby some Lewis acid sites of the zirconia contribute to the total acidity of the catalyst. When comparing the distribution of the sites, one can see that the catalyst based on bare SBA-15 exhibits a majority of medium acid sites (0.214 mmol NH_3 uptake $g_{Cat.}^{-1}$, corresponding to 63%). Conversely, the catalyst based on zirconia-grafted SBA-15 shows a decreased number of medium acid sites (0.199 mmol NH_3 uptake $g_{Cat.}^{-1}$, corresponding to 45%), thus giving rise to an increased number of weak sites (0.086 mmol NH_3 uptake $g_{Cat.}^{-1}$, corresponding to 19%). This shift in the acid strength is explained by electronic interactions between the support and the HPA (Scheme 1). During impregnation with STA, the OH groups at the surface of the support are protonated, leading to a positively charged surface. The addition of HPA then results in an electronic interaction, whereby the strength of the latter depends on the character of the metal oxide support.[14,26] Alsalme et al. recently stated that metal oxide supports (e.g., niobia, zirconia, and titania) significantly decreased acid strength of supported HPAs with regard to a silica support.[27,28]

Table 2. Amount of acid sites of supports and catalysts used.[a]

Sample	NH_3 uptake [mmol $g_{Cat.}^{-1}$] (relative amount [%]) total	weak	medium	strong
bare SBA-15	0.004	0.0005 (10)	0.0035 (90)	0.0000 (0)
ZrO_2 on SBA-15	0.178	0.068 (38)	0.051 (29)	0.059 (33)
STA on SBA-15	0.339	0.018 (5)	0.214 (63)	0.107 (32)
STA on ZrO_2/SBA-15	0.442	0.086 (19)	0.199 (45)	0.157 (36)

[a] Desorption temp.: weak 100–300 °C; medium 300–450 °C; strong >450 °C.

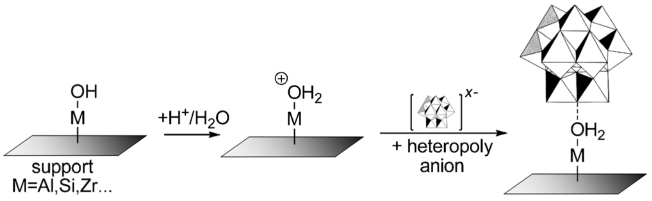

Scheme 1. Electronic interaction between a Keggin-type heteropolyanion and metal oxide support.

Thermogravimetric analysis of fresh catalyst

The thermal stability of STA supported on bare SBA-15 and zirconia-grafted SBA-15 was determined by means of thermogravimetric analysis (TGA) under air. From the curves shown in Figure 2, one can see that both samples exhibit a characteristic loss of crystalline water between 100 and 150 °C. When STA was supported on bare SBA-15, a second loss of 1.1%—with reference to the initial weight—was observed starting from 300 °C. Such behavior can be ascribed to the loss of constitutional water, according to Scheme 2. However, STA supported on zirconia-grafted silica exhibits no loss at high temperature, implying that HPA remained intact. This stabilization of STA when supported on zirconia-modified silica was ascribed to electronic interactions between HPA and the support (Scheme 1). As initially stated for the acidity, the electronic interactions between STA and zirconia were stronger than those with silica, whereby the thermal stability increased because cleavage of constitutional water necessitated breaking of these electronic bonds.[28]

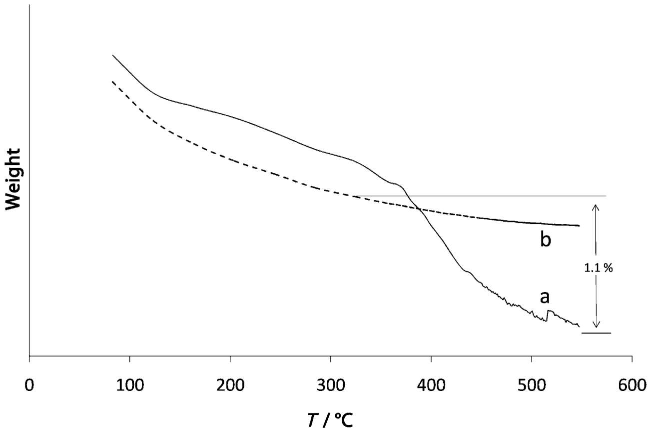

Figure 2. Weight loss of STA supported on a) SBA-15 and b) zirconia-grafted SBA-15.

$$H_4SiW_{12}O_{40}\ n\ H_2O \underset{<200°C}{\overset{-\,n\ H_2O}{\rightleftharpoons}} H_4SiW_{12}O_{40} \underset{>300°C}{\overset{-\,2\ H_2O}{\rightleftharpoons}} SiW_{12}O_{38} \xrightarrow[>500°C]{} 12\ WO_3 + SiO_2$$

Scheme 2. Sequence of reactions leading to the thermal decomposition of STA.

Thermogravimetric analysis of spent catalyst

The spent catalyst containing STA on bare silica was analyzed by means of TGA under air after 25 h of reaction to determine the optimum temperature for oxidative regeneration. From the weight profile, one can see that the catalyst loses significant mass starting from 300 °C (Figure 3). This loss cannot only be explained by the cleavage of constitutional water because the relative change in mass is quantified at 18.0% (vs. 1.1% initially observed for the fresh catalyst). One can thereby ascribe this decrease to the decomposition of the deposited carbonaceous species issued from the dehydration reaction. This is further confirmed by the strong exothermic peak at 420 °C observed by means of differential scanning calorimetry (Figure 3). As a second intermediate conclusion, one can state that the optimum temperature for the oxidative regeneration of the catalyst is higher than 300 °C. This also implies that oxidative regeneration will inevitably result in the loss of constitutional water from STA when supported on bare SBA-15, which is considerably less the case when supported on zirconia-grafted SBA-15 due to its aforementioned increased thermal stability (cf. Figure 3).

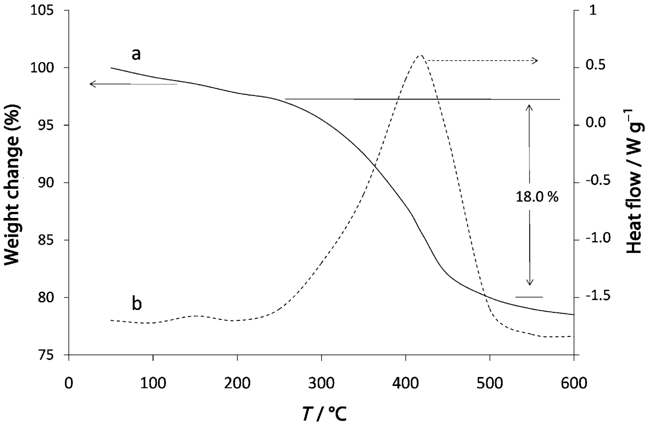

Figure 3. a) TGA and b) differential scanning calorimetry of spent catalyst (STA on bare SBA-15).

Characterization of the coke deposit

The type of coke deposit on the spent catalyst was further determined by using ^{13}C NMR spectroscopy and GC–MS measurements. For the latter technique, pure THF was added to the spent catalyst (ZrO_2-grafted and ZrO_2-free supported catalysts), and the liquid phase was analyzed. The resulting chromatograms exhibited a large number of small peaks, but only one major signal. From the resulting mass spectrum (Figure 4), we attempted to identify the product using the NIST spectral database. The proposed molecules (Figure 4) generally exhibit the presence of aromatic cycles and oxygen-containing functional groups (hydroxyl, acetate, methoxyl, and carboxyl groups). Nevertheless, none of the proposed molecules were plausibly explained with regard to established reaction schemes, although the formation of aromatic molecules from acetone and allylic alcohol was already postulated by Corma et al.[18] Furthermore, as the technique was limited to THF-soluble carbonaceous species, some types of coke, for example, graphite-like carbon, remained unidentified; a fact that was even visibly detected because the THF-washed catalyst remained dark.

Following GC–MS, both types of spent catalysts (ZrO_2-grafted and ZrO_2-free catalyst) were analyzed by means of ^{13}C NMR spectroscopy. The spectra exhibit three massive bands at $\delta=30$, 65, and 130 ppm. Similar spectra were reported in the literature for spent zeolite catalysts used in catalytic cracking.[29,30] The corresponding bands were ascribed to aliphatic ($\delta=20$–80 ppm) and aromatic molecules ($\delta=100$–160 ppm). Hereby, the aliphatic signal was more pronounced in the region of $\delta=50$–90 ppm, which indicated the presence of heteroatomic carbon supposedly originating from oxygenated species (C_{ali}–O). Furthermore, the small band at around $\delta=20$–30 ppm was identified as $-CH_2$ and $-CH_3$ groups. Altogether, this was in agreement with the proposed molecules from GC–MS analysis (Figure 5).

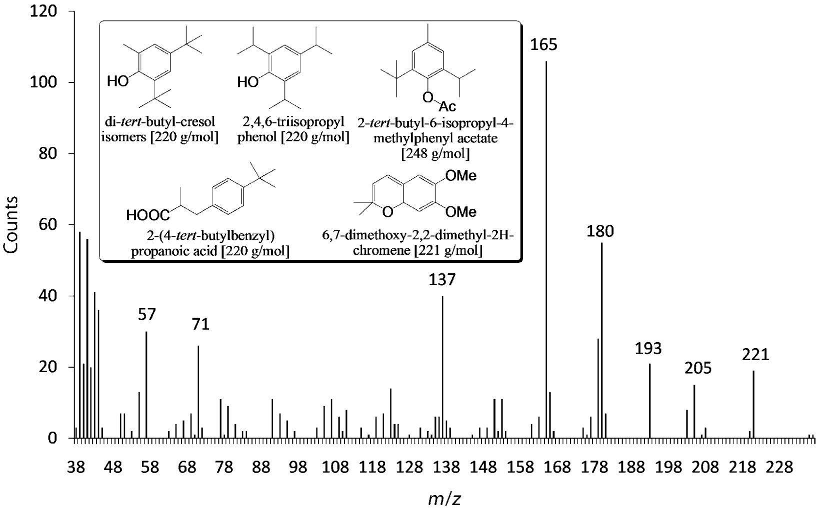

Figure 4. Mass spectrum of the major peak obtained in GC–MS analysis of the spent catalyst.

FTIR spectroscopy

The presence of STA before and after catalytic tests was further studied by means of IR spectroscopy. From the spectra (Figure 6), one can see that all catalysts exhibit characteristic

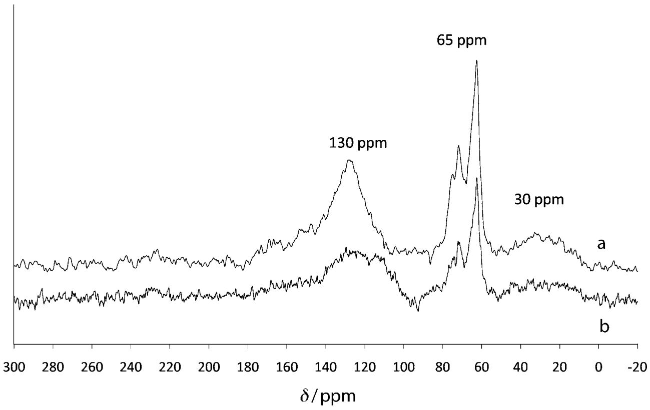

Figure 5. ^{13}C NMR spectra of spent catalyst based on a) bare silica and b) ZrO_2-grafted silica.

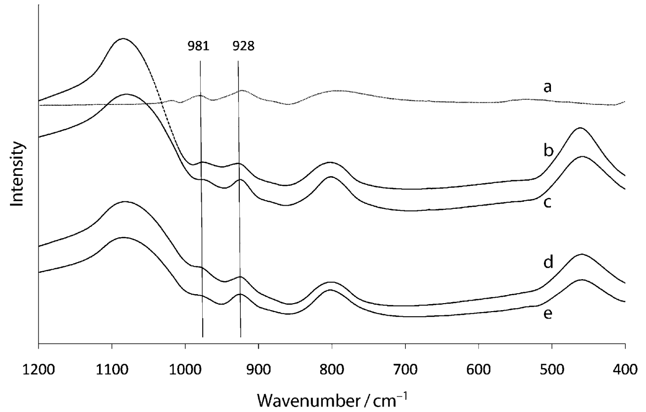

Figure 6. FTIR spectra for bulk STA (a), STA on fresh (c) and spent (b) SBA-15, STA on fresh (e) and spent (d) ZrO_2-grafted SBA-15.

absorption bands of the STA Keggin unit at $\tilde{\nu} = 981$ and 928 cm^{-1}, which were attributed to the symmetric stretching of the addenda atom–terminal oxygen bond (W=O) and the asymmetric stretching of the central atom–oxygen bond (Si–O), respectively.[31] Because these signals were even detected for the spent catalysts (after 25 h of reaction), one can suppose that the active phase remains essentially intact during the reaction. Nevertheless, partial decomposition cannot be excluded because the amounts of the corresponding products would be low, and therefore, remain below the limit of detection.

Catalytic tests

Initial catalytic performance and regeneration in dry and wet air

The initial catalytic performance and deactivation of STA on SBA-15 and STA on ZrO_2-grafted SBA-15 catalysts were studied during 25 h of reaction. From Table 3, one can see that both catalysts give 71 % yield of acrolein during the first 5 h of reaction. After 25 h of reaction, the catalytic activity of both catalysts is significantly decreased, which is attributed to the deposition of coke on the surface of the catalyst (cf. TGA of spent catalyst in Figure 3). The conversion of STA on bare silica is more than halved (41 % vs. 84 % initially), whereas the zirconia-containing catalyst has lost only one fifth of its initial activity (78 vs. 96 % initially). Comparable results were also reported by Kim et al. using the same type of catalyst on zirconia.[32] This phenomenon is ascribed to the reduced acid strength of STA when using strong Lewis acids as supports (cf. acidity of fresh catalysts, Scheme 1).[26] The reduced acid strength results in less carbon deposit, and therefore, increased long-term catalytic performance. In the next step, both catalysts were regenerated in situ, meaning that the catalysts were left inside the reactor after the reaction to directly perform the regeneration process. Therefore, the inlet feed was replaced with air (20 mL min^{-1}), and the reactor temperature was kept at 275 °C to enable regeneration while avoiding the decomposition of STA (cf. TGA of fresh catalyst in Figure 2). After 6 h of regeneration under air, the catalytic performance was determined again. From Table 3, one can see that only the catalyst containing zirconia nearly recovered its initial performance, exhibiting 89 % conversion (vs. 96 % initially) and 78 % of yield in acrolein (vs. 71 % initially). The catalyst based on bare silica also showed a higher catalytic activity than before regeneration with 60 % conversion versus 41 % after 25 h, but its initial activity (84 % of conversion) was not recovered in this case. Furthermore, the yield of acrolein after the regeneration cycle was

Table 3. Catalytic performance tests (blank test results are given in Table S1 in the Supporting Information).[a]

	Reaction time		Regeneration		Periodic regeneration[d]	
	0–5 h (0–1 h)	24–25 h	dry[b]	wet[c]	24–25 h	96–97 h
20 wt % STA on SBA-15						
C[e] [%]	84 (86)	41	60	64	90	87
S_{AC}[f] [%]	83 (79)	57	50	66	84	85
S_{HA}[g] [%]	5 (5)	5	4	7	3	5
Y[h] [%]	71 (68)	24	30	42	76	74
CB[i] [%]	91 (86)	85	72	83	88	91
20 wt % STA on ZrO_2/SBA-15[j]						
C[e] [%]	96 (98)	78	89	86	78	76
S_{AC}[f] [%]	74 (38)	88	88	89	45	46
S_{HA}[g] [%]	12 (17)	12	11	11	12	16
Y[h] [%]	71 (37)	69	78	77	35	35
CB[i] [%]	96 (56)	100	99	100	67	71

[a] Operating conditions: 275 °C reaction temperature; 0.3 g catalyst, 220 h^{-1} gas hourly space velocity of glycerol (gly); STA = silicotungstic acid ($H_4SiW_{12}O_{40}$). [b] 6 h in dry air at 275 °C. [c] 6 h in wet air at 275 °C; molar ratio $N_2/O_2/H_2O = 0.78:0.17:0.05$. [d] Isochronical reaction and regeneration cycle of 10 min. [e] C = conversion of glycerol. [f] S_{AC} = selectivity to acrolein. [g] S_{HA} = selectivity to acetol. [h] Y = yield in acrolein. [i] CB = carbon balance. [j] ZrO_2 amount 20 wt %.

only slightly higher than before (30 vs. 24%), which implies that the catalyst lost some selectivity to acrolein. This result is ascribed to thermal decomposition of STA in hot spots resulting from exothermal oxidative combustion of the deposited carbon. As the thermal stability of STA decreased when supported on bare silica, this phenomenon was only observed for the zirconia-free catalyst. Nevertheless, because no decomposition of the active phase in the spent catalyst was detected by means of FTIR spectroscopy (cf. Figure 6), we decided to modify the regeneration conditions to hinder the thermal decomposition reaction of the catalyst (Scheme 1) by introducing steam into the regeneration feed (equilibrium displacing). Therefore, the two fresh catalysts were again used in the dehydration reaction for 25 h. The regeneration was then performed under steam-enriched air by replacing the glycerol feed with water (molar ratio $N_2/O_2/H_2O = 0.78:0.17:0.05$), whereas the reactor temperature remained unchanged. Similar to the case for dry air, the catalyst based on zirconia-grafted SBA-15 recovered its initial performances. Conversely, the zirconia-free catalyst again did not recover its initial catalytic activity (64% conversion vs. 84% initially). Nevertheless, one can state in this case that the yield of acrolein is significantly higher when regeneration is performed in steam-enriched air (42 vs. 24% in a dry atmosphere). This result suggests that, as expected, the thermal decomposition of STA was at least partially inhibited, which may be explained by 1) the increased heat capacity of steam, leading to lower hot-spots, and 2) the shift of the equilibrium of the decomposition reaction (Scheme 2) to the left side due to the presence of water, as proposed by several researchers.[33,34]

As far as STA on ZrO_2-grafted SBA-15 catalyst is concerned, one can see that there is no effect at all from the presence of water in the regenerative atmosphere, which is consistent with the aforementioned explanation. Indeed, as shown by TGA (cf. Figure 3), STA exhibits increased thermal stability when supported on zirconia-grafted SBA-15, whereby no decomposition takes place under the conditions applied during the regeneration process. Accordingly, the addition of water during regeneration has no impact at all.

Periodic regeneration experiments

The experiments using periodic regeneration of the catalysts are based on the aforementioned idea of using a spare reactor, where the spent catalyst is regenerated in parallel to the running reactor. Therefore, the catalysts were left under stream for 5 h before starting to alternate the reactant and regeneration flows with an interval time of 10 min for each flow. As seen from the previous experiments, the presence of steam during regeneration had no effect on the subsequent catalytic performance of the zirconia-containing catalyst, and even the positive impact in the case of the zirconia-free catalyst was rather low. As the latter did not recover its initial performance even under a steam-rich atmosphere, the experiments of periodic regeneration were performed with a regeneration feed consisting of dry air. The performance of the catalysts during the periodic regeneration cycles was determined after 24 h and again after 96 h. From the results reported in Table 3, one can see that the catalyst based on zirconia-free silica shows a stable performance with an acrolein yield in the range of 74–76% at a glycerol conversion of 87–90%. At a first glance, these results seem to be in contradiction with the former ones obtained after regeneration in dry air, for which thermal decomposition was observed. Nevertheless, one has to bear in mind that, in contrast to the former series of tests, the catalyst was only reacted for 5 h (vs. 24 h previously) before starting regeneration. Thereby, the rather limited quantity of deposited carbon results in fewer hot spots, which explains the decreased thermal decomposition of this catalyst.

The catalyst based on zirconia-grafted silica exhibits rather low catalytic performance with no more than 35% yield of acrolein and a glycerol conversion in the range of 76–78%. Once again, this result seems to be in contradiction with the former performance of this catalyst after regeneration. This behavior was ascribed to the important activation period of the catalyst. Whereas the catalyst based on nongrafted silica showed initially high performance even during the first hour under stream (Table 3; 68% yield in acrolein), the catalyst based on zirconia-grafted silica showed rather low performance during start up, which was owied to decreased selectivity to acrolein (38%). Comparable observations were also reported by Chai et al. for zirconia-supported phosphotungstic acid and also for niobium oxide.[10,12,35] More recently, Lauriol-Garbay et al. stated an important activation period when using zirconium–niobium mixed oxides.[36] Even though there is still work required to shed light on a mechanistic explanation for this effect, one can presume that the presence of Lewis acid sites from zirconia is responsible for this behavior. Alhanash et al. proposed an activation mechanism for Lewis acid sites that explained the increased selectivity towards acetol generally observed for Lewis acid catalysts (Scheme 3).[9] It is then this pronounced activation effect that explains the low catalytic performance of the zirconia-containing catalyst when using short reaction cycles (10 min) in contrast to the previous reported results obtained when using a long reaction cycle of 24 h.

Conclusions

The use of zirconia-grafted silica as a support for STA significantly increases the thermal stability of the active phase (reduction of the constitution water loss), whereby the regeneration of the spent catalyst by means of oxidative combustion of coke was made possible. The initial catalytic performance was almost fully recovered, implying that no thermal destruction of the HPA compound took place. Conversely, when using bare silica as a support for STA, the latter exhibits rather low thermal stability. Thereby, the regeneration of the spent catalyst did not result in complete recovery of the initial catalytic performance. Nevertheless, in this case, the presence of water in the regeneration flow showed a positive impact on the catalytic performance of the regenerated catalyst. This is ascribed to partial inhibition of the thermal decomposition of the HPA by equilibrium displacement. Furthermore, the catalysts were

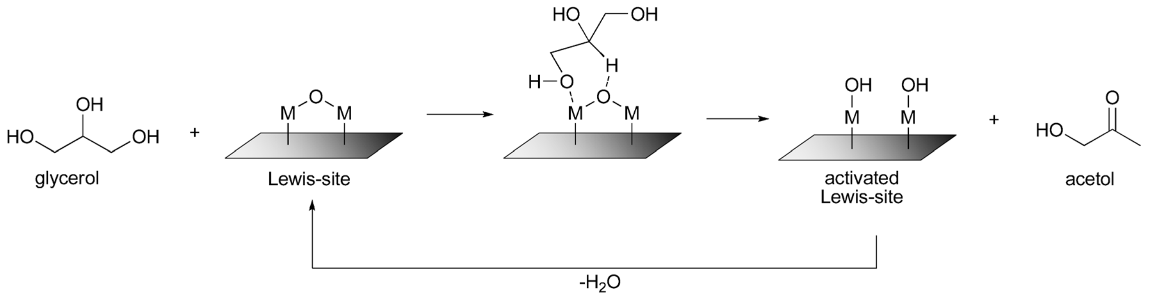

Scheme 3. Mechanistic explanation for the activation period observed for Lewis acid catalysts.[9]

tested under alternating feed cycles of glycerol and air. Due to the short cycle time of 10 min, the catalyst based on zirconia-free silica exhibited a higher performance; a fact explained by the absence of an activation period in this case.

One can, therefore, divide the catalysts into two classes: 1) Brønsted acid catalysts with initially high selectivity to acrolein, but suffering from a short catalyst lifetime; and 2) Lewis acid catalysts with a significant activation period, but increased long-term performance. With regard to these results, the regeneration processes are significantly different for each class of catalyst. Due to the short activation period, Brønsted acid catalysts can be employed in fluidized catalytic bed reactors, similar to the fluidized catalytic cracking process, with a short contact time in the reaction zone. Conversely, the optimal regeneration process for Lewis acid catalysts is similar to a moving bed process, such as that used in catalytic reforming. Hereby, the residence time of the catalyst in the reaction section is in the range of hours or days, whereby the activation period of the catalyst becomes negligible.

Experimental Section

Catalyst preparation

Two types of catalysts were prepared for this study. Both catalysts contained 20 wt% silicotungstic acid (STA, $H_4SiW_{12}O_{40}$) supported either on bare SBA-15 or on zirconia-grafted SBA-15 (final composition: 20 wt% STA, 16 wt% ZrO_2, 64 wt% SiO_2)

Preparation of SBA-15 mesoporous silica: The SBA-15 mesoporous silica support was prepared according to the procedure described by Roggenbuck et al.[37] Accordingly, triblock copolymer P123 (3.25 g; $EO_{20}PO_{70}EO_{20}$, Pluronic P123; Aldrich) were dissolved in a mixture of distilled water (101 mL) and hydrochloric acid (8.7 mL, 37 wt%; Fluka) at 40 °C. Then, tetraethyl-*ortho*-silicate (TEOS; 6.5 g, purity $\geq$99%; Aldrich) was added (resulting in a molar ratio of TEOS/P123/HCl/H_2O = 1.0:0.018:3.3:191). The reaction mixture was stirred for another 24 h at 40 °C, then transferred to a Teflon-coated autoclave and heated for hydrothermal treatment over 24 h at 140 °C. After filtration, the silica was washed with distilled water and dried in air at 80 °C. Finally, calcination was performed in static air at 650 °C for 3 h (heating ramp of 1 $K\,min^{-1}$).

Zirconia grafting: The preparation of the zirconia-grafted SBA-15 was performed by using zirconium(IV) propoxide as an organic precursor for zirconia. The experimental protocol is as follows: SBA-15 support (0.8 g) was slurried in dry ethanol (10 mL; anhydrous, Riedel). Zirconium(IV) *n*-propoxide (0.76 g, 70 wt% solution in *n*-propanol; Aldrich) was added to the mixture, corresponding to an equivalent of 0.2 g of ZrO_2 after hydrolysis. The slurry was left under stirring for another 8 h to hydrolyze the organic zirconia precursor. Then, the solid was filtered off, washed with dry ethanol, and dried in air at 80 °C. Calcination was performed in static air at 650 °C for 3 h (heating ramp of 1 $K\,min^{-1}$) to remove the remaining organic compounds. The corresponding support exhibited an experimental zirconia content of 18.1 wt% versus 20 wt% calculated theoretically, which is explained by the washing of the support prior to drying and calcination.

Impregnation with STA: The impregnation with STA was performed as follows. STA (0.2 g; Sigma) was added to a slurry of support (0.8 g) in water (20 mL). The mixture was subsequently stirred for another 2 h before the water was evaporated under vacuum. The obtained catalyst was dried in air for 24 h at 70 °C before use. The final catalyst particle size was $<$100 mesh.

Characterization techniques

Nitrogen adsorption/desorption isotherms were obtained at −190 °C by using a Micromeritics ASAP 2010 analyzer. The specific surface area (S_{BET}) was determined by using the Brunauer–Emmett–Teller (BET) method, and the pore size distribution was calculated according to the Barret–Joyner–Halenda (BJH) formula. The total pore volume (V_p) was determined by using the value measured at a relative pressure (P/P_0) of 0.995. Before measurement, the samples were outgassed under vacuum at 140 °C for 3 h.

Temperature programmed desorption of NH_3 (NH_3-TPD) was used to characterize the acidity in terms of amount and strength of the acid sites. The experiments were performed by using a Micromeritics AutoChem II 2920 apparatus connected to a mass spectrometer (Varian). The samples were first degassed at 300 °C before being flushed three times with NH_3 at 100 °C. Afterwards, NH_3 desorption was performed with a temperature ramp of 10 $K\,min^{-1}$ up to 550 °C and detected by using a thermal conductivity detector (TCD) and a mass spectrometer.

The thermal stability of the supported STA and the efficiency of the oxidative regeneration of the spent catalyst were evaluated by interpreting thermogravimetric measurements performed on a Micromeritics AutoChem II 2920 apparatus. The samples (about 20 mg) were initially treated with a helium flow for 1 h at 100 °C to remove physisorbed water. Then, the samples were heated to 500 °C under air (5 $K\,min^{-1}$) while recording the weight loss. In the case of the spent catalyst, the thermogravimetry was coupled with differential scanning calorimetry to monitor the heat flow from the oxidative combustion of coke.

The IR spectra were recorded for samples in pressed KBr tablets by using a spectrometer equipped with a mercury cadmium telluride (MCT) detector. The nominal spectral resolution was 4 $\mathrm{cm^{-1}}$ and 256 scans (acquisition time 52 s) were accumulated for each spectrum. A KBr spectrum was used as a background sample for post-processing.

The nature of the carbon species deposited on the spent catalyst was determined by performing ^{13}C NMR spectroscopy using a Bruker spectrometer at an operating frequency of 100.6 MHz. Furthermore, the deposited carbon was further analyzed by means of GC–MS measurements: THF was added to the spent catalyst, and the suspension was stirred for 1 h before the liquid phase was analyzed by means of GC–MS using a Varian 3800 gas chromatograph associated to a Varian Saturn 2000 mass spectrometer.

Catalytic reaction

The catalytic performance was determined at atmospheric pressure for 300 mg of catalyst in a tubular fixed-bed reactor (8.1 mm diameter, 100 mm length) at a reaction temperature of 275 °C. The reaction setup is shown in Figure 7. The glycerol solution (10 wt %) was fed by means of an HPLC pump (Gilson) at a flow rate of 1.5 $\mathrm{mL\,h^{-1}}$. The solution was evaporated in a homemade evaporator placed in a heated box (210 °C). The glycerol vapors were further diluted in a flow of 30 $\mathrm{mL\,min^{-1}}$ inert carrier gas (nitrogen) regulated by a mass flow controller (Brooks). The reaction mixture was then fed to the reactor, which was located in a separate compartment. During the stabilization period of the glycerol feed (12 h), the reaction mixture bypassed the reactor. Downstream of the reactor, the condensable products were collected for 1 h in one of the two parallel ice traps (initially filled with 10 g of water), whereby an uninterrupted sampling of the products was possible by swapping. The mass balance of the traps was always greater than 97 %.

For the regeneration experiments, the setup was further equipped with a second feeding line for air, also regulated by a mass flow controller (Brooks). The airflow (1.2 $\mathrm{mL\,h^{-1}}$) was either introduced by passing through the evaporator or just behind the latter through valve 1, which is a two-position, four-way sampling valve (ViciValco). The first path was used to enrich the regeneration flow with steam, whereas the second path provided the possibility of a periodic permutation between air and reactant flow, for which the valve was actuated by a motor commanded by a PC to control the time of each cycle.

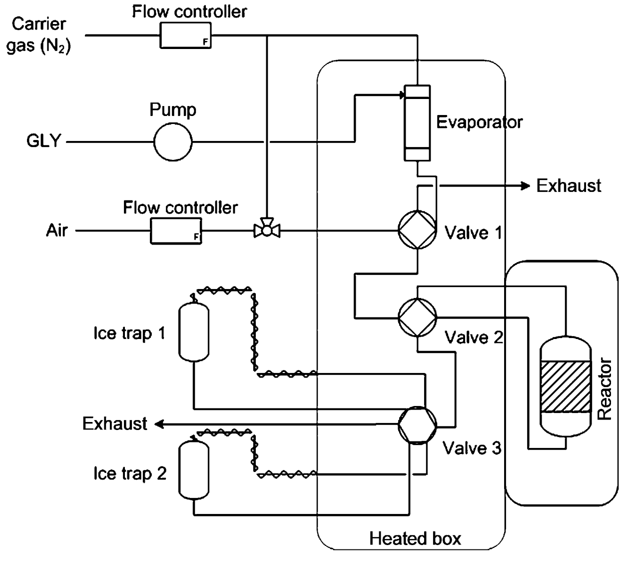

Figure 7. Reaction setup for alternating the glycerol and air feed by a periodical switch of valve 1.

The detailed procedure of regeneration was as follows: prior to the catalytic test, the glycerol feed was stabilized while bypassing the reactor. After 12 h of stabilization, glycerol was fed to the catalyst for 25 h to determine the initial performance. Afterwards, the glycerol feed was stopped while maintaining helium flow in the reactor. After 1 h, the reactor was again bypassed, whereby the catalyst remained under an inert-gas atmosphere (helium). Then, water was introduced by means of an HPLC pump and diluted in air. The corresponding water/air feed was stabilized for 12 h before being fed to the reactor. After 6 h of regeneration, the HPLC pump was stopped, and the regeneration feed was replaced by helium, whereby the catalyst became flushed with inert gas. Then, the reactor was again bypassed and glycerol was introduced by means of the HPLC pump. After 12 h of stabilization of the glycerol feed, the dehydration reaction was restarted to determine the catalytic performance after regeneration. Due to the complexity of the process, it was not adaptable for pulsed regeneration.

The content of the traps was analyzed by performing HPLC using a THERMO SpectraSystem with a Phenomenex Rezex ROA organic acid $\mathrm{H^+}$ column (250 mm length, 7 μm particle size) as a stationary phase and an aqueous solution of sulfuric acid (5 $\mathrm{mmol\,L^{-1}}$; 0.5 $\mathrm{mL\,min^{-1}}$; isocratic) as an eluting agent. For detection, the system was equipped with a refractometer (THERMO Surveyor Plus RI). The catalytic performances (conversion of glycerol C_{gly}, selectivity S_{N}, yield Y_{N}) were calculated by using Equations (1)–(3):

$$C_{\mathrm{gly}}\ (\%) = \frac{\mathrm{mol_{gly,\ reactant\ feed}} - \mathrm{mol_{gly,\ outlet\ feed}}}{\mathrm{mol_{gly,\ reactant\ feed}}} \times 100\,\% \tag{1}$$

$$S_{\mathrm{N}}\ (\%) = \frac{\mathrm{mol_{C\ in\ prod.,\ reactant\ feed}}}{\mathrm{mol_{C\ in\ gly,\ reactant\ feed}} - \mathrm{mol_{C\ in\ gly,\ outlet\ feed}}} \times 100\,\% \tag{2}$$

$$Y_{\mathrm{N}}\ (\%) = C_{\mathrm{gly}}\ (\%) \times S_{\mathrm{N}}\ (\%) \tag{3}$$

The selectivity was reported for acrolein and acetol. Other identified products were acetaldehyde, propionaldehyde, acetone, and allylic alcohol, of which the cumulated selectivity did not exceed 1 %. The carbon balance was determined by taking into account unconverted glycerol in the outlet and the yields of all identified products, which were calibrated by injection of standard solutions.

Acknowledgements

We thank Gerard Cambien for the nitrogen physisorption experiments and Olivier Gardoll for NH_3-TPD and TGA measurements. Furthermore, we thank Adisseo for financial support.

Keywords: acrolein · dehydration · glycerol · heterogeneous catalysis · supported catalysts

[1] A. J. Ragauskas, C. K. Williams, B. H. Davison, G. Britovsek, J. Cairney, A. Eckert, W. J. Frederick, Jr., J. P. Hallet, D. J. Leak, C. H. Liotta, J. R. Mielenz, R. Murphy, R. Templer, T. Tschaplinski, *Science* **2006**, *311*, 484.
[2] A. Corma, S. Iborra, A. Velty, *Chem. Rev.* **2007**, *107*, 2411.

[3] J. N. Chheda, G. W. Huber, J. A. Dumesic, *Angew. Chem.* **2007**, *119*, 7298; *Angew. Chem. Int. Ed.* **2007**, *46*, 7164.
[4] European directive 2003/30/EC of May 8th, **2003**.
[5] B. Katryniok, S. Paul, M. Capron, F. Dumeignil, *ChemSusChem* **2009**, *2*, 719.
[6] B. Katryniok, S. Paul, P. Rey, V. Bellière-Baca, F. Dumeignil, *Green Chem.* **2010**, *12*, 2079.
[7] A. K. Kinage, P. P. Upare, P. Kasinathan, Y. K. Hwang, J.-S. Chang, *Catal. Commun.* **2010**, *11*, 620.
[8] C. J. Jia, Y. Liu, W. Schmidt, A. H. Lu, F. Schüth, *J. Catal.* **2010**, *269*, 71.
[9] A. Alhanash, E. F. Kozhevnikova, I. V. Kozhevnikov, *Appl. Catal. A: Gen.* **2010**, *378*, 11.
[10] S.-H. Chai, H.-P. Wang, Y. Liang, B. Q. Xu, *Green Chem.* **2008**, *10*, 1087.
[11] E. Tsukuda, S. Sato, R. Takahashi, T. Sodesawa, *Catal. Commun.* **2007**, *8*, 1349.
[12] S.-H. Chai, H.-P. Wang, Y. Liang, B. Q. Xu, *J. Catal.* **2007**, *250*, 342.
[13] F. Wang, J.-L. Dubois, W. Ueda, *J. Catal.* **2009**, *268*, 260.
[14] H. Atia, U. Armbruster, A. Martin, *J. Catal.* **2008**, *258*, 71.
[15] J.-L. Dubois, C. Duquenne, W. Hölderich (Arkema), WO 2006087083, **2006**.
[16] A. Ulgen, W. Hölderich, *Catal. Lett.* **2009**, *131*, 122.
[17] J.-L. Dubois, C. Duquenne, W. Hölderich, J. Kervennal (Arkema), WO 2006087084, **2006**.
[18] A. Corma, G. W. Huber, L. Sauvanaud, P. O'Connor, *J. Catal.* **2008**, *257*, 163.
[19] Y. Arita, H. Kasuga, M. Kirishiki (Nippon Catalytic Chem. Ind.), JP 2008110298, **2008**.
[20] J. J. Strohm, A. H. Zacher, J. E. White, M. J. Gray, V. Lebarbier, US2011075743.
[21] R. Galiasso Tailleur, C. Albornoz, *Catal. Today* **2010**, *150*, 308.
[22] S.-H. Chai, H.-P. Wang, Y. Liang, B. Q. Xu, *Green Chem.* **2007**, *9*, 1130.
[23] T. Okuhara, N. Mizuno, M. Misono, *Adv. Catal.* **1996**, *41*, 113.
[24] I. V. Kozhevnikov, *Catalysts for Fine Chemicals, Vol. 2*, **2002**, Wiley, Chichester.
[25] I. V. Kozhevnikov, *J. Mol. Catal. A: Chem.* **2007**, *262*, 86.
[26] B. Katryniok, S. Paul, M. Capron, C. Lancelot, P. Rey, V. Bellière-Baca, F. Dumeignil, *Green Chem.* **2010**, *12*, 1922.
[27] A. M. Alsalme, P. V. Wiper, Y. Z. Khimyak, E. F. Kozhevnikova, I. V. Kozhevnikov, *J. Catal.* **2010**, *276*, 181.
[28] A. Alsalme, E. F. Kozhevnikova, I. V. Kozhevnikov, *Appl. Catal. A: Gen.* **2010**, *390*, 219.
[29] J. L. Bonardet, M. C. Barrage, J. Fraissard, *J. Mol. Catal. A: Chem.* **1995**, *96*, 123.
[30] P. Castaño, G. Elordi, M. Olazar, A. T. Aguayo, A. Pawelec, J. Bilbao, *Appl. Catal. B: Environ.* **2011**, *104*, 91.
[31] R. Thouvenot, M. Fournier, R. Franck, C. Rocchiccioli-Deltcheff, *Inorg. Chem.* **1984**, *23*, 598.
[32] Y. T. Kim, K.-D. Jung, E. D. Park, *Bull. Korean Chem. Soc.* **2010**, *31*, 3283.
[33] Y. Konishi, K. Sakata, M. Misono, Y. Yoneda, *J. Catal.* **1982**, *77*, 169.
[34] I. V. Kozhevnikov, *Handbook of Green Chemistry, Vol. 2*, Wiley-VCH, Weinheim, **2009**.
[35] S.-H. Chai, H.-P. Wang, Y. Liang, B. Q. Xu, *Appl. Catal. A: Gen.* **2009**, *353*, 213.
[36] P. Lauriol-Garbay, J. M. M. Millet, S. Loridant, V. Bellière-Baca, P. Rey, *J. Catal.* **2011**, *280*, 68.
[37] J. Roggenbuck, G. Koch, M. Tiemann, *Chem. Mater.* **2006**, *18*, 4151.

Received: October 11, 2011
Revised: November 12, 2011

B. Katryniok, S. Paul, M. Capron,*
V. Bellière-Baca, P. Rey, F. Dumeignil

■■–■■

Regeneration of Silica-Supported Silicotungstic Acid as a Catalyst for the Dehydration of Glycerol

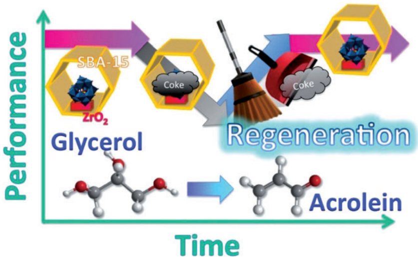

Catalytic support: The regeneration of supported silicotungstic acid, widely used in the dehydration of glycerol to yield acrolein, is described. The nature of the support has a strong impact on the thermal stability of the active phase. Zirconia stabilizes silicotungstic acid, thus enabling efficient and nondestructive regeneration (see picture).